

STABLE ANDREWS–CURTIS CONJECTURE VIA FAKE SURFACES AND ZEEMAN CONJECTURE

LUCAS FAGAN, YANG QIU, AND ZHENGHAN WANG

ABSTRACT. We propose an induction scheme that aims at establishing the stable Andrews–Curtis conjecture in the affirmative. The stable Andrews–Curtis conjecture is equivalent to the conjecture that every contractible fake surface is 3-deformable to a point. We prove that every contractible fake surface of complexity less than 6 is 3-deformable to a point by induction.

1. INTRODUCTION

The stable Andrews–Curtis conjecture (sACC) is an intriguing problem closely related to the smooth 4-dimensional Poincaré conjecture (sPC4) [1]. While sACC is widely believed to be false, no strong evidence has emerged. In this paper, we propose an induction scheme that aims at establishing sACC in the affirmative.

The sACC claims that the space of balanced presentations of the trivial group is connected by several stable Andrews–Curtis moves. Any presentation P of a group π leads to a natural 2-complex K_P whose fundamental group is π . By general position, K_P can be PL embedded into \mathbb{R}^5 . If K_P is contractible, then the boundary of a closed tubular neighborhood $N(P)$ of K_P in \mathbb{R}^5 is a PL homotopy 4-sphere. The stable AC moves correspond to simple homotopy moves on $N(P)$, implying that if P is trivial under stable AC moves, then $N(P)$ is a tubular neighborhood of a point and thus a PL 5-ball. It follows that the boundary PL homotopy 4-sphere $\partial N(P)$ of $N(P)$ is the smooth standard 4-sphere, and thus counterexamples to sPC4 cannot be constructed in this way.

In this paper, we study the topological version of sACC [9]: that every contractible 2-complex 3-deforms to a point. Simple homotopy by expansion and collapse is a stronger form of homotopy equivalence. The Bing house with two rooms is a well-known example of a contractible complex that cannot be collapsed to a point.

Because every 2-complex can be 3-deformed to a fake surface [8], it suffices to prove the sACC by demonstrating that all contractible fake surfaces can be 3-deformed to a point. Our strategy to prove the sACC is to 3-deform contractible fake surfaces to a point by induction on the complexity of the fake surfaces.

We observe that contractible fake surfaces may have a weakness: one of the 2-cells in any contractible fake surface has to be embedded as conjectured in [3], which gives an instability in the presentations of the trivial group. This instability arises from the existence of a relator in which each generator appears at most once. This relator allows us to reduce the number of generators in the presentation by substitutions. We do not know yet how to use this observation directly for proofs, so instead we approach the topological version by reducing the complexity of fake surfaces using embedded disks.

The Zeeman conjecture says that for any contractible 2-complex K , $K \times I$ can be collapsed to a point [10]. The Zeeman conjecture is believed to be false as well, but there are interesting

special cases. In the case of contractible fake surfaces that are embeddable in 3-manifolds [10, 4], the Zeeman conjecture is equivalent to the 3-dimensional Poincaré conjecture, and therefore holds. In the case of contractible fake surfaces that are not embeddable in 3-manifolds, the Zeeman conjecture is equivalent to sACC [7]. Thus by establishing sACC for low complexity, we also prove the Zeeman conjecture for these cases.

We follow strictly the notation and terminology for fake surfaces in our earlier paper [3]. Fake surfaces are generic 2-polyhedra, so they have only two kinds of singularities besides the regular manifold points: a point on an edge where three half planes join (type 1 singularity), and the center of a tetrahedron in the dual cellulation of triangulations of 3-manifolds (type 2 singularity).

We denote by $\mathcal{F}_C(s, t)$ the set of all closed contractible fake surfaces which contain t vertices and whose 1-skeletons have s connected components. Our main result is a proof of the topological version of sACC for surfaces in $\mathcal{F}_C(1, t)$, where $t \leq 5$. The case of complexity $t = 1$ is the main result of [5].

The following is our main result, which is stated more precisely in Theorem 6.

Theorem 1. *Contractible fake surfaces of complexity less than 6 with connected 1-skeletons are all 3-deformable to a point.*

Corollary 2. *Given a contractible cellular fake surface $F = (G, \{c_i\})$ of complexity less than 6 and let T be a maximal tree in G . If T is collapsed to a base point and P is the resulting presentation of the trivial group, then the stable Andrews–Curtis conjecture holds for P .*

Corollary 3. *Let $N(F)$ be a closed regular neighborhood of a cellular fake surface F embedded in R^5 . If the complexity of F is less than 6, then $N(F)$ is the standard 5-ball B^5 .*

Corollary 4. *The Zeeman conjecture holds for any contractible cellular fake surface F of complexity less than 6.*

The proof for surfaces of complexity 1 was given by Ikeda in [5]. Our extension to complexity up to 5 is by induction. We give a method to reduce one fake surface to another one of lower complexity up to complexity 5, then our result follows by induction.

2. THE STABLE ANDREWS–CURTIS CONJECTURE

Definition 5 (Stable Andrews–Curtis Moves). Let $P = \langle x_1, \dots, x_n \mid r_1, \dots, r_n \rangle$ be a balanced group presentation. The *stable Andrews–Curtis moves* are the following:

- (AC1) Replace r_i with $r_i r_j$ for some $j \neq i$
- (AC2) Replace r_i with r_i^{-1}
- (AC3) Replace r_i with $g r_i g^{-1}$ where g is a generator or its inverse
- (AC4) Add a new generator x_{n+1} and trivial relator $r_{n+1} = x_{n+1}$
- (AC5) Remove a trivial relator and the generator, i.e., the inverse of (AC4)

The stable Andrews–Curtis conjecture allows for two additional moves beyond the usual AC-moves (AC1)–(AC3).

Two presentations are said to be *stably Andrews–Curtis equivalent* if one can be obtained from the other by a finite sequence of moves (AC1)–(AC5).

A presentation is said to be *stably Andrews–Curtis trivial* if it is stably Andrews–Curtis equivalent to the trivial presentation $\langle \mid \rangle$.

Using these moves, we can state the stable Andrews–Curtis conjecture:

Conjecture (Stable Andrews–Curtis Conjecture). *Every balanced presentation of the trivial group is stably Andrews–Curtis trivial.*

The stable Andrews–Curtis conjecture also has a topological formulation [9], which is what our approach relies on:

Conjecture (Topological Version of sACC). *Every contractible 2-complex 3-deforms to a point.*

Since every 2-complex 3-deforms to a fake surface, sACC is also equivalent to the conjecture that every contractible fake surface 3-deforms to a point.

3. EMBEDDED DISK MOVES

In this section, we introduce the main technical tool used in this paper: two moves that 3-deform a closed fake surface with an embedded disk, depending on whether the embedded disk has a trivial or nontrivial T -bundle. In particular, we obtain a new surface by collapsing the union of the old surface and a 3-ball along a disk. We call these the *trivial embedded disk move* and *nontrivial embedded disk move*, respectively.

We also introduce some conventions that we use in the remainder of the paper. For a fake surface F , we define $\mathcal{S}_n(F)$ to be the set of type n singularities of F . In particular, $|\mathcal{S}_2(F)|$ is the number of vertices of F .

We use the notation $[x_1, \dots, x_n]$ to represent the attaching map of a disk, where a negative denotes inverse. Similarly, (x_1, x_2, x_3) denotes a part of an attaching map of a disk. In Case 3, we use adjacent disks to give explicit descriptions of T -bundles.

Suppose F_1 is a closed fake surface with an embedded disk D and there are n vertices on the boundary ∂D of D .

3.1. Embedded Disk with Trivial T -Bundle. When the T -bundle over ∂D is trivial, the neighborhood of D in F_1 is as shown in Figure 1, where we represent the edges of 1-skeleton by green lines, vertices in $\mathcal{S}_2(F_1)$ by black points, D by the blue disk. Denote by A the annulus above D and with one boundary component attached to ∂D and the other boundary component indicated by the red circle in Figure 1. Set $J = D \cup A$. Then J is a disk embedded in F_1 , and $J \times I$ is a 3-ball topologically. We denote by E the 3-polyhedron obtained by attaching $J \times I$ to F_1 such that $J \times 0 = J$.

As shown in Figure 2, $J \times I$ consists of n 3-subpolyhedrons whose 1-faces are indicated by red and blue lines. They are all 3-balls topologically. Now we collapse these 3-balls along certain 2-faces to get a new closed fake surface F_2 . First, we collapse the 3-ball indicated by the left diagram in Figure 2 along the free 2-face enclosed by red lines. Next we collapse the other 3-balls indicated by the right diagram in Figure 2 by pushing upwards the 2-faces enclosed by red lines. We call this sequence of 3-deformations the *trivial embedded disk move*.

When $n \geq 2$, we get a new closed fake surface locally as shown in Figure 3. The original vertices A_1 and A_2 are removed and new vertices A'_3, \dots, A'_n are introduced, so the new surface F_2 contains $|\mathcal{S}_2(F_1)| + n - 4$ vertices.

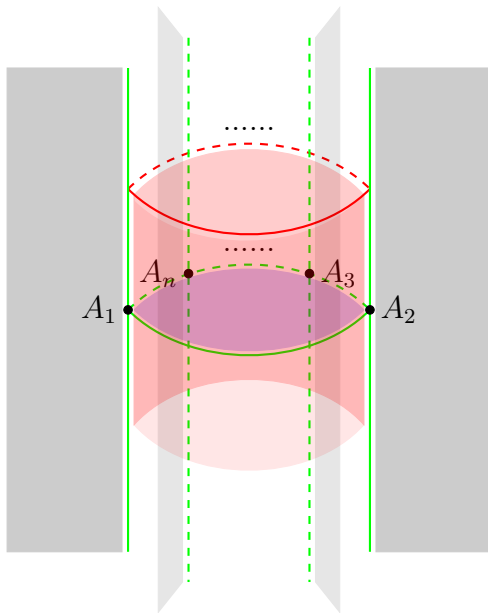


FIGURE 1. Neighborhood of D in F_1 for Trivial T -Bundles

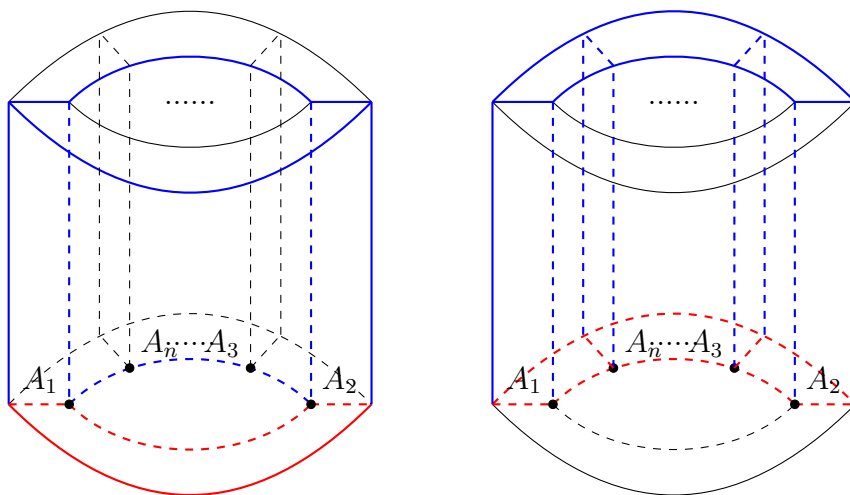


FIGURE 2. $J \times I$ for Trivial T -Bundles

In particular, for $n = 2$, the number of vertices decreases by 2: $|\mathcal{S}_2(F_2)| = |\mathcal{S}_2(F_1)| - 2$. Green edges are separated into two disjoint parts locally as shown in Figure 3. Thus F_2 may have one more connected component in its 1-skeleton than F_1 . For $n = 3$, the number of vertices decreases by 1. Green edges are still connected together, so F_2 has the same number of connected components of 1-skeleton as F_1 . In this case, the move is simply the T^{-1} move from [8].

When $n = 1$, the collapses above introduce a free 1-face as indicated by the red line in Figure 4. Collapsing the disk containing this free 1-face may increase the number of

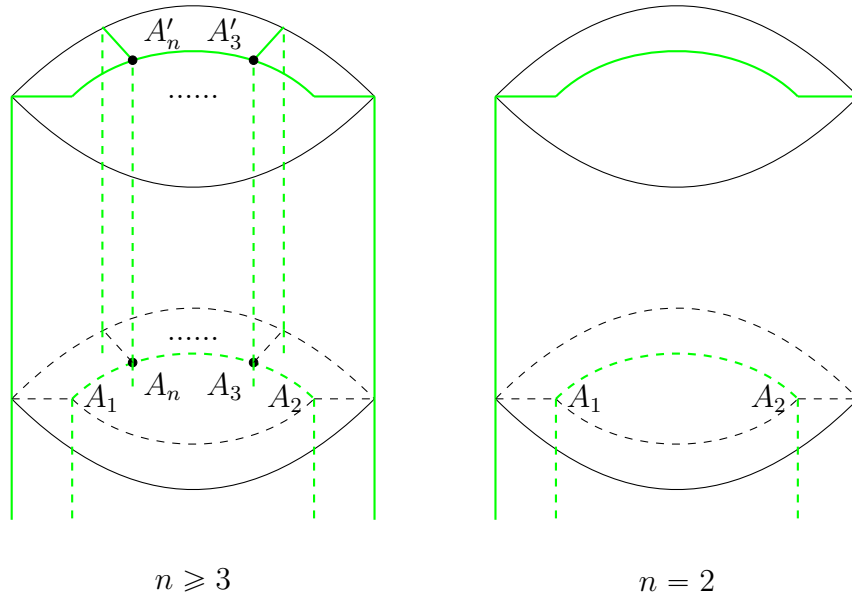


FIGURE 3. F_2 for Trivial T -Bundles

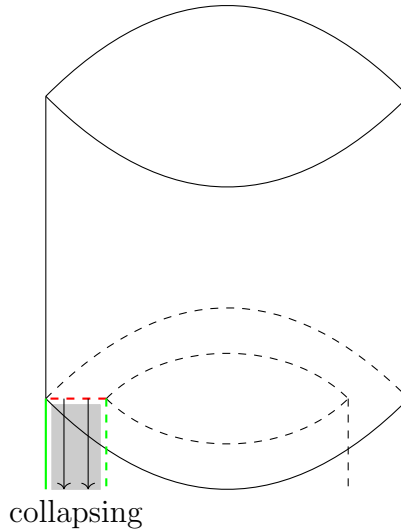


FIGURE 4. F_2 with Free 1-Face for $n = 1$

connected components of the 1-skeleton. If the complexity is greater than 1, the embedded disk D must contain a vertex other than A_1 . Thus $|\mathcal{S}_2(F_2)| \leq \max\{|\mathcal{S}_2(F_1)| - 2, 0\}$.

The effect of this move is shown in Figure 5. The maximal case in which the complexity is reduced, i.e., when $n = 3$, is shown in Figure 6. As mentioned above, in this case the move is equivalent to the T^{-1} move from [8].

3.2. Embedded Disk with Nontrivial T -Bundle. When the T -bundle over ∂D is nontrivial, the neighborhood of D in F_1 is as shown in Figure 7. Denote by B the upper band of

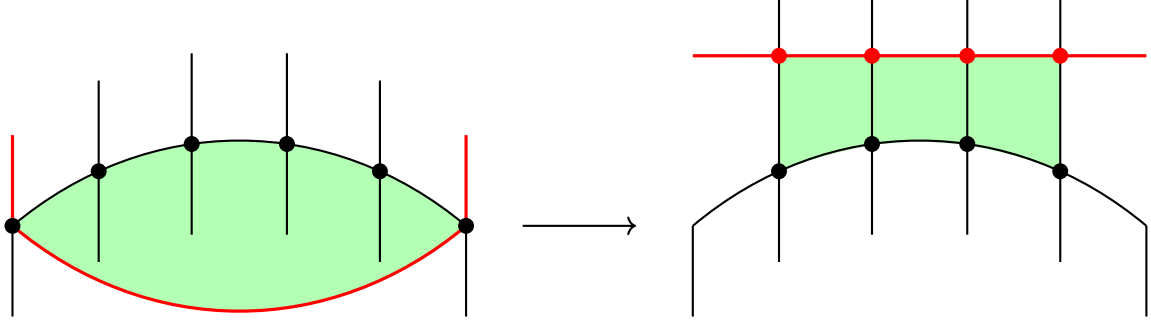


FIGURE 5. The trivial embedded disk move. Embedded disks are colored, with green indicating they have trivial T -bundles. After applying the move, two vertices are removed, and $n - 2$ new vertices are created.

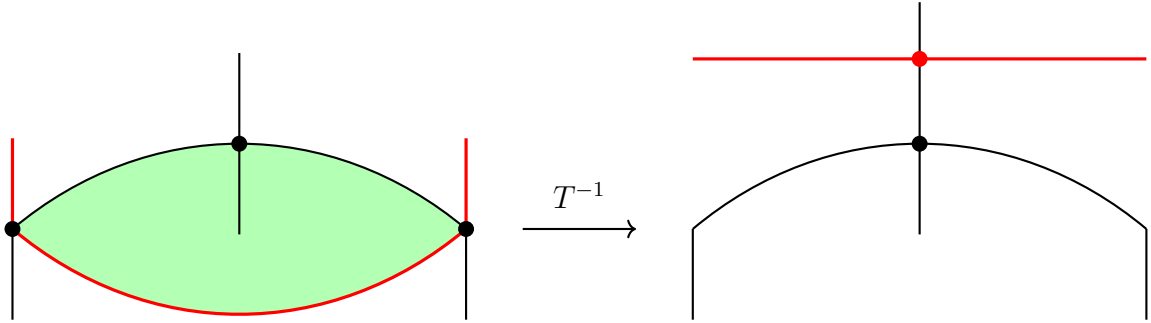


FIGURE 6. The trivial embedded disk move in the case $n = 3$. This is the maximal case in which the complexity is reduced. In this case, the move is equivalent to the T^{-1} move from [8].

the Möbius band, where one long edge is attached to ∂D and the other long edge is indicated by the red line in the bottom diagram in Figure 8. Set $J = D \cup B$. Then J is an embedded disk in F_1 as shown in Figure 8. Attach 3-ball $J \times I$ to F_1 along $J \times 0 = J$ to get E .

As shown in Figure 9, $J \times I$ consists of n 3-balls whose 1-faces are indicated by red and blue lines. Similarly to the case of trivial bundles, we collapse E to get F_2 as follows. First, we collapse the 3-ball indicated by the left diagram in Figure 9 along the free 2-face enclosed by red lines. Next, we collapse the other 3-balls indicated by the right diagram in Figure 9 by pushing upwards the 2-faces enclosed by red lines. We call this sequence of 3-deformations the *nontrivial embedded disk move*.

When $n \geq 2$, we get a new closed fake surface indicated by the left diagram in Figure 10. The original vertex A_2 is removed and new vertices A'_3, \dots, A'_n are introduced. The original vertex A_1 remains, unlike in the case of trivial bundles, so the new surface F_2 contains $|\mathcal{S}_2(F_1)| + n - 3$ vertices.

In particular, for $n = 2$, the number of vertices decreases by 1. Green edges are still connected together, so F_2 has the same number of connected components of 1-skeleton as F_1 . In this case, the move is simply the U^{-1} move from [8]. Note that for $n = 3$, the number of vertices is unchanged.

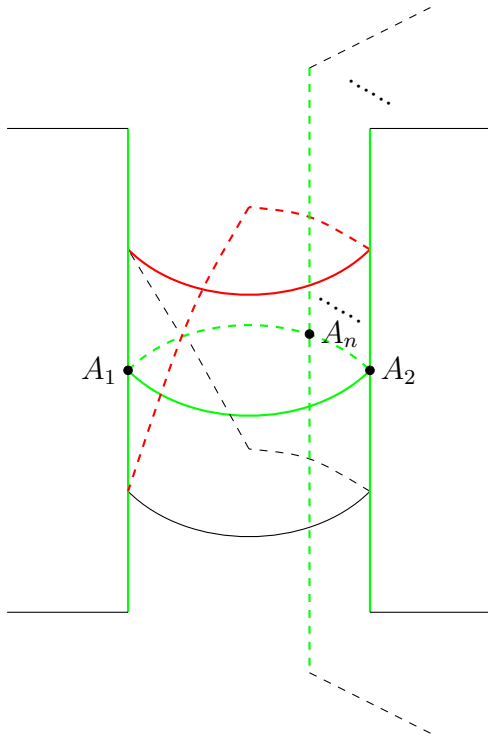


FIGURE 7. Neighborhood of D in F_1 for Nontrivial T -Bundles

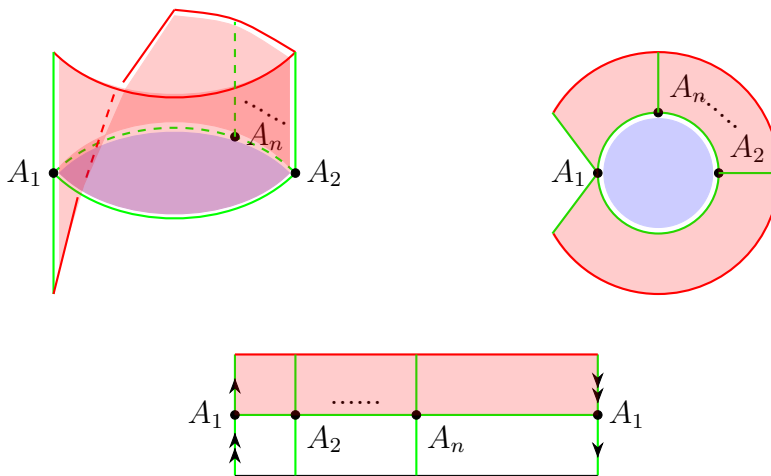


FIGURE 8. J for Nontrivial T -Bundles

When $n = 1$, we get a closed surface F_2 indicated by the right diagram in Figure 10. The original green circle $\partial D \subset \mathcal{S}_2(F_1)$ is changed to a dashed circle which represents a circle in a region. The other two remaining green edges are connected. Thus F_2 has the same number of connected components of 1-skeleton as F_1 . The unique original vertex A_1 is removed, and so F_2 contains one fewer vertex than F_1 .

In the remainder of the paper, we refer to these two moves the *trivial embedded disk move* and the *nontrivial embedded disk move*. When we apply these moves to an embedded disk,

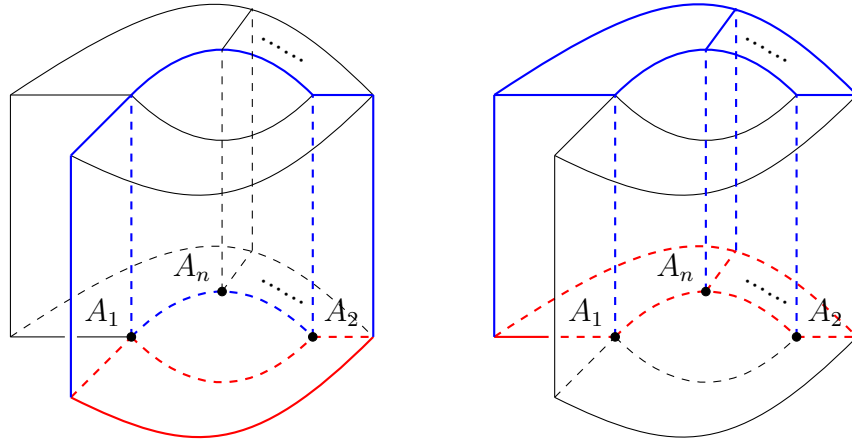


FIGURE 9. $J \times I$ for Nontrivial T -Bundles

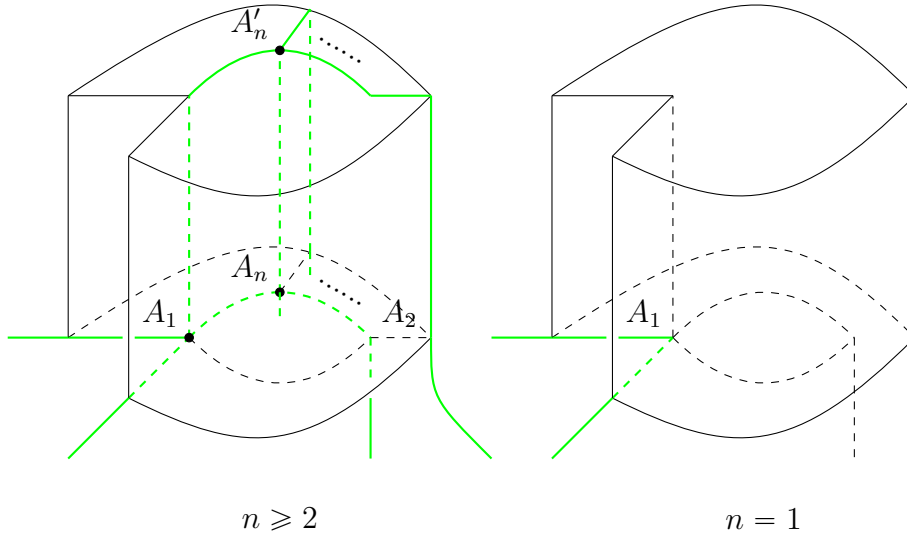


FIGURE 10. F_2 for Nontrivial T -Bundles

we say that we do so “along” an edge, which refer to the edge(s) of the embedded disk that are removed.

4. REDUCING THE COMPLEXITY OF A FAKE SURFACE

In this section, we prove the following theorem, which is the main result of this work:

Theorem 6 (Precise statement of Theorem 1). *For any surface $F \in \mathcal{F}_C(1, t)$ where $t \leq 5$, there exists a zigzag*

$$F \swarrow F_1 \searrow F_2 \swarrow \dots \searrow F_{n-1} \swarrow F_n \searrow *$$

of elementary collapses, each either leftwards or rightwards, such that $\dim(F_i) \leq 3$.

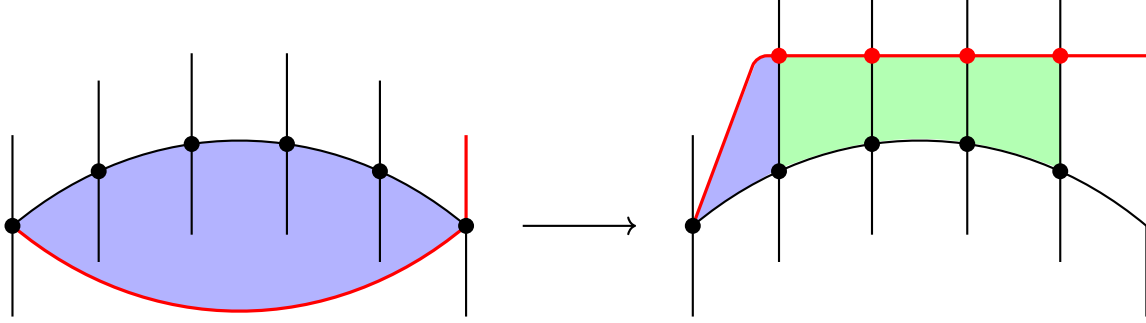


FIGURE 11. The nontrivial embedded disk move. Embedded disks are colored, with green indicating a trivial T -bundle and blue indicating a nontrivial T -bundle.

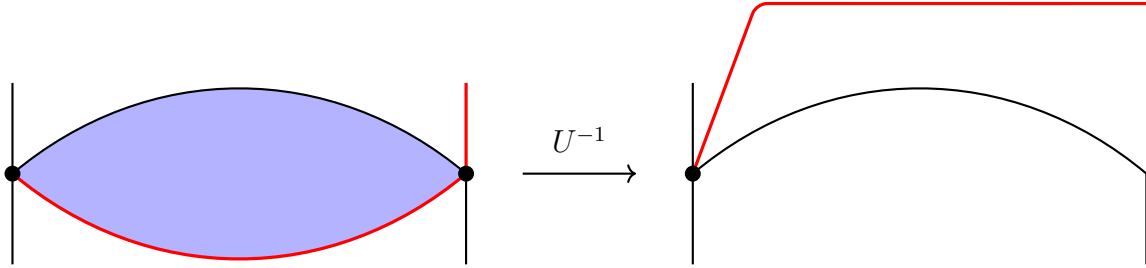


FIGURE 12. The nontrivial embedded disk move in the case $n = 2$. This is the maximal case in which the complexity is reduced. In this case, the move is equivalent to the U^{-1} move from [8].

4.1. **Complexity Reduction Lemma.** We begin by proving a lemma consisting of conditions under which a fake surface can be reduced in complexity.

Lemma 7 (Complexity Reduction Lemma). *A fake surface F can be 3-deformed to another fake surface of lower complexity if F satisfies one of the following criteria:*

- 1) F contains an embedded disk with at most three vertices and a trivial T -bundle.
- 2) F contains an embedded disk with at most two vertices and a nontrivial T -bundle.
- 3) F contains two embedded disks with three vertices that share exactly one vertex.
- 4) F contains one embedded disk with 3 vertices and another embedded disk with 3 or 4 vertices, and the two embedded disks share exactly one edge.
- 5) F contains an embedded disk with 4 vertices and trivial T -bundle and another disk with 4 vertices, and either the two disks share exactly two non-adjacent edges or the embedded disk intersects the other disk in one edge twice. If the second disk has a trivial T -bundle, then the condition that two edges are non-adjacent can be removed.
- 6) F contains an embedded disk with 4 vertices and trivial T -bundle, another disk with 4 vertices that intersects the embedded disk in two consecutive edges, and another disk with 4 or 5 vertices as in Figures 16 and 17.

- 7) F contains an embedded disk with 5 vertices and trivial T -bundle and another embedded disk with 4 vertices and trivial T -bundle, and the two disks share exactly two non-adjacent edges.
- 8) F contains an embedded disk with 5 vertices and trivial T -bundle and three disks with 4 vertices as in either Figures 19 or 20.

Our proof of the complexity reduction lemma goes case by case as follows.

Cases 1 and 2. Cases 1 and 2 follow directly from applying the trivial embedded disk move and nontrivial embedded disk move described in Section 3.

Case 3. It suffices to consider the case where both embedded disks have nontrivial T -bundles, since otherwise we can reduce the complexity by Case 1. In Figure 13, let the T -bundle of the red disk $[7, -12, 4]$ be given by

$$(3, 7, 15), (-15, -12, 13), (-13, 4, 1), (-1, 7, 16), (-16, -12, 14), (-14, 4, -3),$$

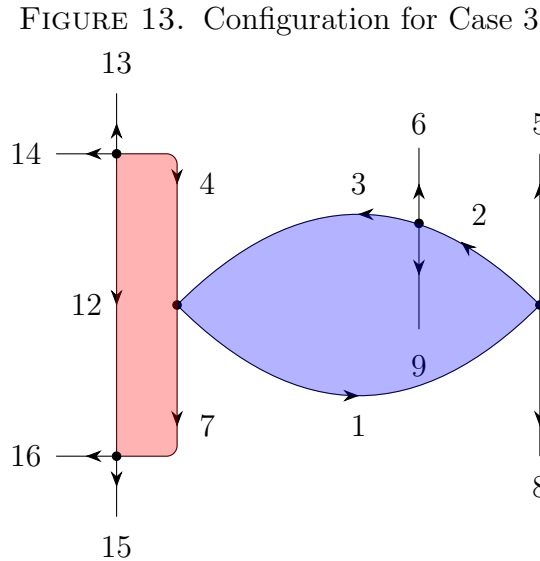
and the T -bundle of the blue disk $[1, 2, 3]$ be given by

$$(4, 1, 5), (-5, 2, 6), (-6, 3, 7), (-7, 1, 8), (-8, 2, 9), (-9, 3, -4).$$

We now apply the nontrivial embedded disk move to the blue disk along edge 2. After applying the move, the red disk becomes another embedded disk with 3 vertices whose T -bundle given by

$$(11, 7, 15), (-15, -12, 13), (-13, 4, -11),$$

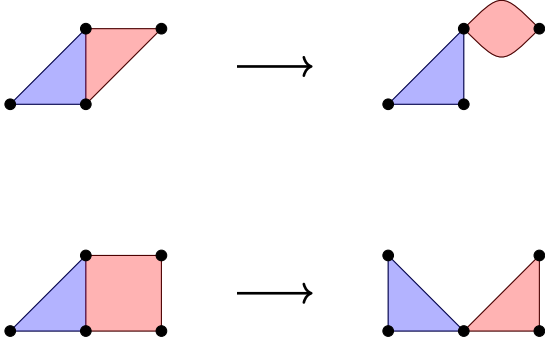
where edge 11 is the new diagonal edge as in Figure 11. This is a trivial T -bundle, so we can reduce the complexity by Case 1.



Two embedded disks with 3 vertices that share exactly one vertex.

Case 4. It suffices to assume that the T -bundle of the blue disk in Figure 14 is nontrivial, since otherwise we can apply case 1. We apply the nontrivial embedded disk move to the blue disk along the shared edge such that the disks are changed to two disks that share exactly one vertex. The two possibilities are shown in Figure 14. In each case, we can apply Case 1, 2, or 3 to reduce the complexity.

FIGURE 14. Configurations for Case 4

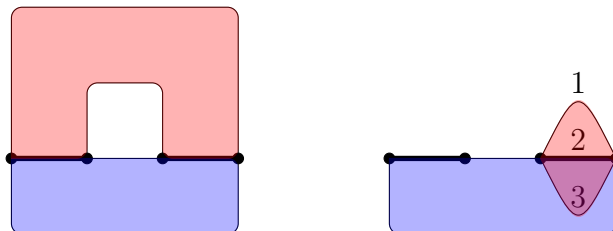


Left: An embedded disk with 3 vertices and an embedded disk with 3 or 4 vertices that share exactly one edge. **Right:** The resulting configuration after applying the nontrivial embedded disk move to the blue disk.

Case 5. The two possible configurations for Case 5 are shown in Figure 15. We apply the trivial embedded disk move to the blue disk along the thickened edges. The red disk will be changed to a disk with 2 vertices, allowing us to reduce the complexity using Case 1 or 2. If the red disk has a trivial T -bundle, the two edges on which the disks intersect can be adjacent. This is because the trivial embedded disk move will not change the triviality of disks, and in the case of adjacent edges, the second disk will become a disk with no more than 3 vertices and trivial T -bundle. Thus we can reduce the complexity using Case 1.

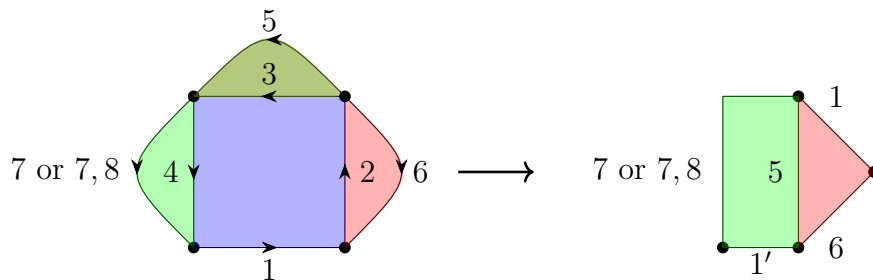
Case 6. The two possible configurations in Case 6 are given in Figures 16 and 17. It is sufficient to assume that the T -bundles of the second and third disks are nontrivial, since otherwise we can reduce the complexity by Case 5. In the first case, shown in Figure 16, we do the trivial embedded disk move with the blue disk $[1, 2, 3, 4]$ along edges 2 and 4. We get an embedded disk with 3 vertices and an embedded disk with 3 or 4 vertices that share exactly one edge, and the resulting fake surface has the same complexity as before. Thus, we can apply Case 4. In the second case, shown in Figure 17, we again do the trivial embedded disk move with the blue disk $[1, 2, 3, 4]$ along edges 2 and 4. This again gives an embedded disk with 3 vertices and an embedded disk with 3 or 4 vertices that share exactly one edge, and again the resulting fake surface has the same complexity as before. We apply Case 4 to reduce the complexity.

FIGURE 15. Configurations for Case 5



Left: Two embedded disks with 4 vertices that share two non-adjacent edges. **Right:** Two embedded disks with 4 vertices where the red disk intersects the blue disk at one edge twice. The red disk's attaching map is $[2, 1, 2, 3]$.

FIGURE 16. First Configuration for Case 6

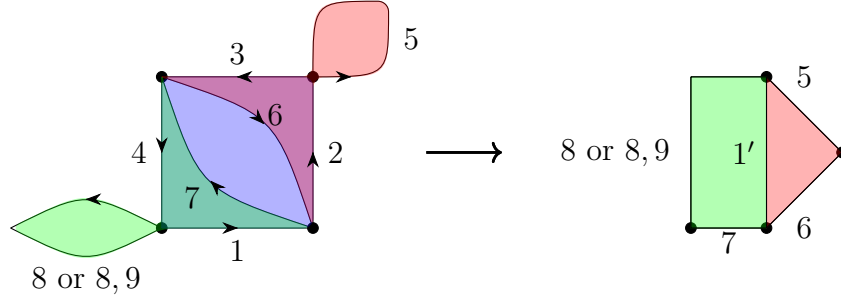


Left: There is an embedded disk $[1, 2, 3, 4]$, a disk $[2, 5, -3, 6]$, and a disk $[-4, -5, 3, 7]$ or $[-4, -5, 3, 7, 8]$. **Right:** The resulting configuration has an embedded disk with 3 vertices and an embedded disk with 3 or 4 vertices that share exactly one edge.

Case 7. The configuration of Case 7 is shown in Figure 18. In this case, we do the trivial embedded disk move to the blue disk with 5 vertices along the thick edges as in Figure 18. This increases the complexity of the resulting fake surface by 1. However, the red disk is changed to a disk with two vertices and trivial T -bundle. We then apply the trivial embedded disk move to this disk, which decreases the complexity by 2. Thus, the resulting surface is of lower complexity than the original one.

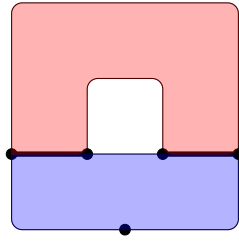
Case 8. The first case is shown in Figure 19. We can assume that $[2, 9, 4, 8]$ and $[10, -3, 9, -3]$ have nontrivial T -bundles, since otherwise we can reduce the complexity by Case 7. We do the trivial embedded disk move to $[1, 2, 3, 4, 5]$ along edges 1 and 3, which increases the complexity by 1. The resulting fake surface has three embedded disks as in the right side of Figure 19, where the green disk with 2 vertices and the red disk with 5 vertices have nontrivial T -bundles. We then do the nontrivial embedded disk move to the green disk to remove edge 9 from the red disk and go back to the original complexity. The new red disk has 4 edges, and so we can apply Case 4 to the new red disk and the gray disk. We can use a similar method for the second case in Figure 20.

FIGURE 17. Second Configuration for Case 6



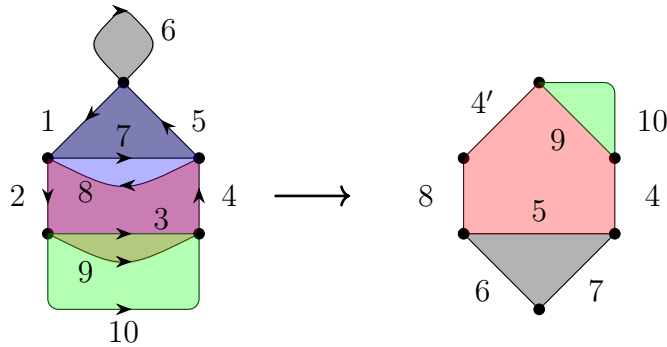
Left: There is an embedded disk $[1, 2, 3, 4]$, a disk $[2, 5, 3, 6]$, and a disk $[1, 7, 4, 8]$ or $[1, 7, 4, 8, 9]$. **Right:** The resulting configuration has an embedded disk with 3 vertices and an embedded disk with 3 or 4 vertices that share exactly one edge.

FIGURE 18. Configuration for Case 7



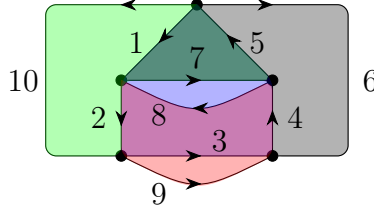
An embedded disk with 5 vertices and an embedded disk with 4 vertices that share two non-adjacent edges.

FIGURE 19. First Configuration for Case 8



Left: There are embedded disks $[1, 2, 3, 4, 5]$, $[1, 7, 5, 6]$, $[2, 9, 4, 8]$, and $[10, -3, 9, -3]$. **Right:** The resulting configuration has an embedded disk with 2 vertices, and embedded disk with 5 vertices, and an embedded disk with 3 vertices.

FIGURE 20. Second Configuration for Case 8



Embedded disks $[1, 2, 3, 4, 5]$, $[10, -2, 7, 5]$, $[2, 9, 4, 8]$, and $[6, 4, -7, -1]$.

4.2. Fake Surfaces with Disconnected 1-Skeleta. Using the classification of contractible fake surfaces up to complexity 5 from [3], it is easy to check that all satisfy one of the conditions of Lemma 7. Thus, we can always 3-deform each surface to another of lower complexity. However, the classification is for fake surfaces with connected 1-skeleta. When we apply the reduction to lower complexity, we may get a fake surface whose 1-skeleton has 2 connected components. We henceforth use $\mathcal{F}_C(s, t)$ to refer to contractible fake surfaces of complexity t whose 1-skeleton has s connected components.

As discussed in the proof of Lemma 7, only the trivial embedded disk move to embedded disks with one or two vertices from Case 1 may give a fake surface in $\mathcal{F}_C(2, t)$. In this case, the number of vertices will decrease by at least 2. Thus, it remains to address the case of $\mathcal{F}_C(2, t)$ for $t \leq 3$.

In [5], it is shown the fake surfaces in $\mathcal{F}_C(2, 1)$ satisfy the stable Andrews–Curtis and the Zeeman conjectures, so it remains to deal with the fake surfaces in $\mathcal{F}_C(2, 2)$ and $\mathcal{F}_C(2, 3)$.

By Lemma 2.9 in [6], each surface $F \in \mathcal{F}_C(2, 3)$ can be constructed in one of the following two ways:

Case 1. In this case, we construct a fake surface $F = F_1 \# F_2$ where $F_1 \in \mathcal{F}_C(1, 2)$ and $F_2 \in \mathcal{F}(1, 1)$ such that $H_1(F_2) = 0$ and $H_2(F_2) = \mathbb{Z}$. Here, $\#$ represents the connected sum of two fake surfaces along their regions. It is straightforward to check that there are three possibilities for F_2 . Their attaching maps are as follows, attached onto the 1-skeleton in Figure 21:

Fake Surface 1: $[-2, 1, 1], [1, 2], [2]$

Fake Surface 2: $[-2, -1, 2, 1], [2], [1]$

Fake Surface 3: $[-2, 1, -2, -1], [2], [1]$

If F_2 is the first fake surface above, through computation about homology groups, the connected sum between F_1 and F_2 can not be done along the unique embedded disk [2] of F_2 . Thus $F = F_1 \# F_2$ contains at least one embedded disk with one vertex such that we can reduce the complexity. When F_2 is either of the other two surfaces, we can always reduce the complexity since both of the surfaces contain two embedded disks.

Case 2. In this case, $F = F_1 \cup F_2$, where F_1 is obtained by removing one disk in the interior of a 2-cell of one surface in $\mathcal{F}_C(1, 3)$, and F_2 is obtained by attaching the boundary of a disk to the center of a Möbius band. F_1 and F_2 are attached along their boundaries. We can

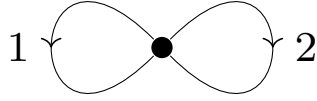


FIGURE 21. 1-Skeleton for F_2

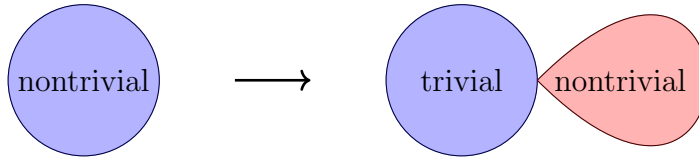


FIGURE 22. Applying Inverse of Nontrivial Embedded Disk Move

collapse F_2 as follows: the 1-skeleton of F_2 is a circle disjoint from the 1-skeleton of F_1 . Based on the construction of F_2 , F_2 contains an embedded disk with the circle as the boundary and the T -bundle of the disk is nontrivial, as shown by the left blue disk in Figure 22. We apply the inverse of the nontrivial embedded disk move, called the loop move in [8], to the blue disk. The blue disk becomes a disk with one vertex and trivial T -bundle. Finally, we do the trivial embedded disk move to the new blue disk and remove the connected component of 1-skeleton of F .

We can apply the same argument to the two ways to construct the surfaces $F \in \mathcal{F}_C(2, 2)$, following the construction in [6], and use the same method to reduce.

Thus, we can use Lemma 7 to reduce each $F \in \mathcal{F}_C(1, t) (1 < t \leq 5)$. When a reduction takes us outside $\mathcal{F}_C(1, t)$, we can use the above method to make it return to $\mathcal{F}_C(1, t)$ or reduce to a point.

This completes the proof of Theorem 6 in all cases.

5. ALGORITHMIC 3-DEFORMATIONS OF FAKE SURFACES

In this section, we provide pseudocode for implementing the embedded disk moves in Algorithms 1 and 2 and a search algorithm to explore 3-deformations of fake surfaces in Algorithm 3. For more details, see [2].

Our goal is to apply the embedded disk moves in order to execute a computer search to 3-deform fake surfaces to spines or ones of lower complexity. While computer exploration has not yielded any new results so far, we plan to continue this approach in the future.

Algorithm 1 Trivial Embedded Disk Move

```

1: function TRIVIALEDMOVE( $S, D, e$ )
2:   Assert that  $D$  is a trivial bundle
3:   Let  $e$  be the front edge; list remaining edges as back edges
4:   Determine all perpendicular edge pairs using adjacency
5:   Introduce new vertical and horizontal edges
6:   Construct a replacement dictionary describing local edge substitutions
7:   Apply all replacements throughout the surface  $S$ 
8:   Remove the original disk  $D$ 
9:   Insert the new disks created by the move geometry
10:  Update edge indices and metadata
11:  return modified surface  $S$ 
12: end function

```

Algorithm 2 Nontrivial Embedded Disk Move

```

1: function NONTRIVIALEDMOVE( $S, D, e$ )
2:   Assert that  $D$  has a nontrivial  $T$ -bundle
3:   Let  $e$  be the front edge; list back edges
4:   Compute perpendicular edge pairs, alternating orientation at each step
5:   Introduce new vertical, horizontal, and diagonal edges
6:   Build the replacement dictionary encoding the move
7:   Apply all replacements across  $S$ 
8:   Remove the original disk  $D$ 
9:   Insert the structured family of disks defined by the move
10:  Remove boundary edges and update metadata
11:  return modified surface  $S$ 
12: end function

```

ACKNOWLEDGMENTS

Y.Q. is supported by National Key R&D Program of China (2024YFA1013202) and Nankai Zhide Foundation. Z.W. is partially supported by ARO MURI contract W911NF-20-1-0082.

REFERENCES

- [1] J. J. Andrews and M. L. Curtis. Free groups and handlebodies. *Proceedings of the American Mathematical Society*, 16(2):192–195, 1965.
- [2] L. Fagan. *The Stable Andrews–Curtis Conjecture and Generic 2-Polyhedra*. Ph.D. thesis, University of California, Santa Barbara, Dec. 2025.
- [3] L. Fagan, Y. Qiu, and Z. Wang. Classification of cellular fake surfaces. *arXiv preprint arXiv:2406.09439*, 2024.

Algorithm 3 Best-First Search Over Fake Surfaces

```
1: function SEARCH( $S_0, T, k$ )  $\triangleright T = \text{max iterations, } k = \text{moves sampled per expansion}$ 
2:   Initialize priority queue  $Q$ 
3:   Compute score of  $S_0$  (complexity, number of nontrivial bundles)
4:   Insert (score,  $S_0, \emptyset$ ) into  $Q$ 
5:   Track  $S_{\text{best}} \leftarrow S_0$  and its score
6:   for  $t = 1$  to  $T$  do
7:     if  $Q$  is empty then
8:       return  $S_{\text{best}}$ 
9:     end if
10:    Pop best surface  $(-, S, H)$  from  $Q$ 
11:    Determine all possible moves on  $S$ 
12:    Sample up to  $k$  moves
13:    for all sampled moves  $m$  do
14:       $S' \leftarrow$  apply trivial or nontrivial embedded disk move  $m$  to a copy of  $S$ 
15:      if  $S'$  is valid then
16:        Compute score of  $S'$ 
17:        Insert (score,  $S', H + [m]$ ) into  $Q$ 
18:        if score( $S'$ )  $\leq$  score( $S_{\text{best}}$ ) then
19:           $S_{\text{best}} \leftarrow S'$ 
20:        end if
21:      end if
22:    end for
23:  end for
24:  return  $S_{\text{best}}$ 
25: end function
```

- [4] D. Gillman and D. Rolfsen. The zeeman conjecture for standard spines is equivalent to the poincaré conjecture. *Topology*, 22(3):315–323, 1983.
- [5] H. Ikeda. Acyclic fake surfaces. *Topology*, 10(1):9–36, 1971.
- [6] Y. Koda and H. Naoe. Shadows of acyclic 4-manifolds with sphere boundary. *Algebraic & Geometric Topology*, 20(7):3707–3731, 2020.
- [7] S. Matveev. Zeeman’s conjecture for unthickened special polyhedra is equivalent to the andrews-curtis conjecture. *Siberian Mathematical Journal*, 28(6):917–928, 1987.
- [8] S. Matveev. *Algorithmic topology and classification of 3-manifolds*, volume 9. Springer, 2007.
- [9] P. Wright. Group presentations and formal deformations. *Transactions of the American Mathematical Society*, 208:161–169, 1975.
- [10] E. C. Zeeman. On the dunce hat. *Topology*, 2(4):341–358, 1963.

DEPARTMENT OF MATHEMATICS, UNIVERSITY OF CALIFORNIA, SANTA BARBARA, CA 93106, USA
Email address: lucasfagan@math.ucsb.edu

CHERN INSTITUTE OF MATHEMATICS AND LPMC, NANKAI UNIVERSITY, TIANJIN, CHINA
Email address: yangqiu@nankai.edu.cn

DEPARTMENT OF MATHEMATICS, UNIVERSITY OF CALIFORNIA, SANTA BARBARA, CA 93106, USA
Email address: zhenghwa@math.ucsb.edu